Vries, S.B. de, Loonen, R. C. G. M. & Hensen, J. L. M., 2019. Sensor selection and control strategy development support for automated solar shading systems using building performance simulation, in Proc. of the 16th International IBPSA Conference (Building Simulation 2019), Rome, 8p.

Sensor selection and control strategy development support for automated solar shading systems using building performance simulation

Samuel B. de Vries, Roel C.G.M Loonen, Jan L.M. Hensen

Unit Building Physics and Services, Department of the Built Environment
Eindhoven University of Technology, the Netherlands

Abstract

This study presents a method for supporting control strategy development and sensor selection for automated solar shading systems from a building physics perspective using building performance simulation (BPS) and gives recommendations for quality assurance in making modelling decisions. With the proposed method high performance sensor strategies (sensor type, its location and actuation thresholds) can be identified using only a limited number of simulations. The method is illustrated using sensor selection for a sun-tracking control strategy for indoor roller blinds as a case study. It is concluded that the daylighting and energy performance of such a strategy can significantly be improved through the application of this method.

Introduction

BPS has been identified as a promising tool for supporting the exploration of high potential control strategies for automated solar shading systems as it allows the operational performance and risks of such strategies to be explored in a wide variety of cases (Loonen et al. 2017). Many recent studies have used simulations to analyse and improve the performance of advanced control strategies for a range of automated shading types (Wienold 2007, Tzempelikos and Shen 2013, Seong et al. 2014, Shen et al. 2014, Gunay et al. 2016, Atzeri et al. 2018). The use of BPS for this application is, however, relatively new and there are several issues that still need to be addressed to ensure effective deployment of BPS in this context.

An example of an advanced control strategy that presents challenges for BPS are strategies for indoor roller blinds with sun tracking behaviour. These systems adapt their position according to the sun path, seeking to balance the admission of daylight and views with the competing goal of limiting daylight glare discomfort and are receiving increasing attention for their potential as key elements in high performance buildings (Koo et al. 2010, Tzempelikos and Shen 2013, Jeong et al. 2016, Atzeri, Gasparella et al. 2018). However, as pointed out by Tzempelikos and Shen (2013) and Atzeri, Gasparella et al. (2018), sun-tracking control strategies do not necessarily eliminate all occurrences of glare and can moreover lead to undesirably high cooling loads. These studies also show that the performance of sun-tracking control strategies can be improved through the application of additional control actions that raise or lower the shade in response to light sensors. In the study by Tzempelikos and Shen (2013) this is done using a proportional control response to an indoor illuminance sensor. The authors proposed a method for developing control thresholds for this response by correlating sensor measurements to desired work plane illuminance ranges.

Different types of sensors could be used for improving a sun-tracking control strategy. The type of sensor that is used, its position and orientation, together with the chosen control thresholds and responses, influence the effectivity of the control strategy in addressing building performance aspects. Generally, complex sensor strategies, in which measurements relate more closely to the physical quantities that directly influence the desired performance aspects, will be more effective. There is, however, also the conflicting desire to keep a control concept as simple as possible. Another consideration is that control rules are easily changed whereas it is undesirable to change sensing equipment once a system has been installed. A need therefore arises to investigate the effectivity of different types of sensor strategies in influencing whole building performance and BPS potentially offers the tools for this.

There are, however, some impediments that hinder the effective application of BPS to the development of advanced control strategies for shading systems in general, and to those tailored to roller blinds specifically. One being that the performance of advanced shading solutions is determined by interactions between the thermal and the daylight domain; two physical domains which are largely separated across different BPS tools. Different methods for overcoming this limitation have been presented. Atzeri, Gasparella et al. (2018) rely on a stepped simulation approach, Loonen (2018) has presented a co-simulation framework and multiple research teams have focussed efforts on developing new simulation environments, tailored for specific advanced fenestration solutions (Shen and Tzempelikos 2012, Bueno et al. 2015, Werner et al. 2017). Computational performance assessment of advanced shading solutions is complicated further by the fact that existing BPS tools offer only a limited degree of control over the behaviour of the shading system (Loonen, Favoino et al. 2017). Most existing simulation methods, for instance, allow a roller blind to only take two discrete positions; being either fully lowered or fully raised. To overcome this limitation, earlier studies have relied on using a limited number of discrete shade positions and dividing the window system into a series of vertically stacked window strips (Wienold

2007, Gunay, O'Brien et al. 2016, Atzeri, Gasparella et al. 2018). Additionally, some researchers have included scripting environments within co-simulation frameworks to facilitate the implementation of a complex control logic (Shen, Hu et al. 2014, Loonen 2018).

From this literature review, it becomes clear that although different approaches for computational performance assessment of advanced dynamic shading systems are available, this field remains in active development and the influence of modelling decisions and resolutions in applying these approaches to advanced sun-tracking control strategies requires further exploration. This paper contributes to the existing body of knowledge on this topic by placing specific emphasis on quality assurance with regards to modelling decisions. A method will be presented for supporting control strategy development and sensor selection from a building physics perspective using only a small number of simulations. The proposed method is illustrated using a sun-tracking control strategy for indoor roller blinds as a case study. In this case study, the merits of three sensor alternatives will be evaluated.

In the following section, the case study and the applied simulation framework will be presented. Using this framework, the performance of an initial version of the control strategy, without any light sensors, will be evaluated in relation to a series of reference scenarios. Through an analysis of whole building performance in relation to sensor measurements, a set of improvements will then be proposed for each of the sensor alternatives. Finally, the potential of these improvements will be evaluated in relation to a conventional control strategy.

Case study and simulation method

Sun tracking control strategy for indoor roller blinds

This case study focusses on evaluating the merits of different sensor alternatives for improving the performance of a sun-tracking control strategy for roller blinds. The initial control strategy, titled solar cut-off (SC), seeks to balance the admission of daylight and views with the competing goal of limiting daylight glare discomfort. To this end, the roller blind is controlled in relation to the sun's position to block direct sunlight from hitting an occupant's desk using the relation shown in Eq.1. The edge of an occupant's desk is assumed to be at 75 centimetres height and positioned 75 centimetres from the façade. If the sun is not in direct view of the façade, the shade is fully raised. This control mode is based on the control strategy proposed by Tzempelikos and Shen (2013).

$$\frac{wpd}{\cos\gamma} \cdot \tan\alpha + wph = sh \qquad (1)$$

wpd: distance between workplane and façade, wph: height of workplane, γ: solar azimuth (west from south convention), α: solar altitude.

This study evaluates the effectivity of three sensor types, in improving the discussed control strategy: (i) an outdoor sensor for global horizontal irradiance, (ii) an outdoor sensor for global vertical irradiance and (iii) an indoor sensor for vertical illuminance. The placement of these sensors is illustrated in Figure 1. The outdoor irradiance sensors are chosen as this type of sensor is commonly installed for integration in building management systems and placed on the rooftop of buildings. The indoor illuminance sensor is positioned in between the glazing and roller blind. This sensor and positioning is chosen because it is considered to be a non-intrusive, low-cost solution. Using this selection of sensors, the importance of both the positioning of a sensor and the part of the solar spectrum it measures, will be tested.

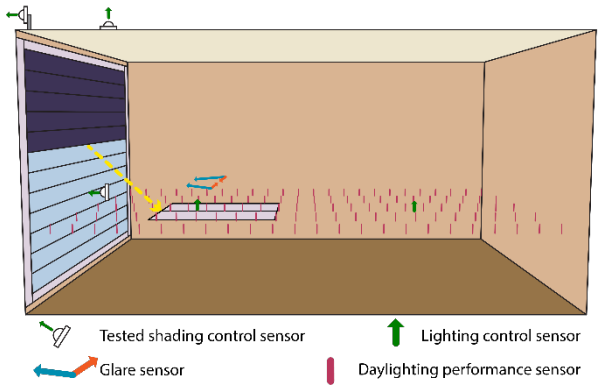

Figure 1 Overview of the set-up of the simulation study.

A conventional control strategy will be used as a reference. In this baseline strategy (BS), the roller blind is controlled using an outdoor global vertical irradiance sensor where the shade is either fully raised or lowered in response to a threshold of 200 W/m^2 (Beck et al. 2010). In addition to this BS a situation where the shades are always up (AU) and a situation with the shades always down (AD) are presented as a reference.

This study uses the reference office building for building integrated solar envelope systems, developed within IEA SHC Task 56 (D'Antoni et al. 2019) with some minor adjustments. Details of this reference space and the associated modelling assumptions are given in Table 1. Although the sun tracking control algorithm can be applied to any façade orientation, this case study is limited to a south facing perimeter office cell.

Performance indicators

The performance aspects of interest in this study are daylight quality, visual comfort, view to the outdoors, and energy efficiency. Spatial daylight autonomy is used as an indicator for daylight quality, with 300 lux and 50% of occupied hours as cut-off criteria (sDA300/50%). This indicator is defined as the percentage of floor area that receives at least 300 lux for more than 50% of the occupied hours.

Visual comfort is operationalised as the lack of visual discomfort and daylight glare probability simplified (DGPs) is used as a performance indicator. This metric, which was empirically derived by Wienold (2009) relates the probability of the occurrence of glare to vertical illuminance at the eye of the observer. Seating arrangements closest to the window are the most sensitive to the occurrence of glare. Additionally the likelihood of glare discomfort is strongly influenced by viewing direction. In this study, the two seating positions shown

in Figure 1; with the view direction facing the window at 45 degrees, are used to assess glare probability. Here the percentage of occupied hours that a DGPs of 0.40 is exceeded (disturbing glare) is used as a performance indicator using the maximum of both viewing positions. View to the outdoors is assumed to be only dependent on the position of the shade. It is assessed as the percentage of occupied hours that the shade is positioned above the eye level of a seated occupant (1.2 meters). Energy efficiency is expressed in terms of primary energy consumption for cooling, heating and lighting and computed using the efficiencies shown in Table 1.

The simulation method and assumptions

To account for the strong dependence of performance on interactions between the thermal and visual domains, this study relies on a co-simulation framework using Radiance (daylighting), EnergyPlus (thermal domain), Matlab (control logic) and BCVTB (information exchange).

In this framework, the Radiance three-phase method is used for daylighting and glare performance assessments as well as the prediction of indoor lighting energy consumption and heat gains. This approach has been validated for the performance assessment of advanced solar shading systems (McNeil and Lee 2013). To simulate a variable height shading system using this method, the fenestration system needs to be divided into a number of horizontally oriented segments which are either fully shaded or unshaded (Subramaniam 2017). All Radiance daylighting simulations are executed before the co-simulation process takes place. In this step, a database is created containing the daylighting contributions of each segment of the window for all day lit hours of the year and both the shaded, as well as the unshaded states.

BCVTB directs the exchange of information between simulation environments. Matlab is used to describe the behaviour of the shading control logic, compute the current daylighting conditions using the daylight database, as well as the resulting interior gains from artificial lighting which are sent to EnergyPlus. The shading models in EnergyPlus do not allow for partially shaded window states to be directly implemented. Here a similar modelling approach was chosen as with Radiance, where the window is divided into segments.

Hourly weather data for Amsterdam (IWEC) is used in this study. Within EnergyPlus, a 5-min time step is chosen, as a sub-hourly resolution helps to increase the reliability of the heat balance algorithms as well as limit the effect of errors deriving from BCVTB's loosely-coupled co-simulation approach. Within Radiance an hourly time step is chosen to describe sky conditions because of the unavailability of sub-hourly weather data and the uncertainties associated to the creation of synthetic sub-hourly data which will be discussed further in the conclusion section.

Results

Sensitivity analyses: division of the window

The modelling approach, in which the window is split into segments, causes the actual position of the roller blind to be rounded to the height of the nearest segment. The rounding of the shade's position will lead to errors in the predicted flux of visual and thermal radiation.

Table 1Case study details and modelling assumptions

		EnergyPlus	Radiance
Geometry	**Dimensions**	width: 4.5m; depth: 6m; height: 3m (27 m^2), façade oriented south	
	Window to wall ratio:	85%	
Fenestration	**Type:**	Low-E (pos. 3) double glazing with argon cavity filling,	
	Glazing:	U_{gl}: 1.2 W/m^2K U_{frame}: 1.5 W/m^2K, SHGC: 0.62, CEN	T_{vis}: 0.82
	Shade:	T_{sol}: 0.05, R_{vis}: 0.76, $SHGC_{gl+shade}$: 0.26, T_{vis}: 0.05, R_{vis}: 0.74, $T_{vis,gl+shade}$: 0.05	
Facade		Rc = 4.5 m^2K/W	r_{vis} = 0.5
Ceiling, walls, floor		Mixed: heavy weight floor/ceiling, lightweight walls	Ceiling: r_{vis} = 0.8, Wall: r_{vis} = 0.5 Floor: r_{vis} = 0.2
Internal gains	**People:**	3 (variable occupancy). 120 W/pers.	
	Occupancy:	Weekdays: 8:00-19:00 (2860 hours/year)	
	Lighting:	10.9 W/m^2 Dimming (linear between 0-500 lux) Two sensors (Figure 1) each control 50% of loads	
	Equipment:	7.0 W/m^2	
HVAC and settings	**Infiltration:**	ACH: 0.15	
	Ventilation:	Demand driven, 40 m^3/(h*pers.), ACH: 1 (average)	
		Sensible heat recovery, eff.: 70%	Sensor grid: 5x25
	Setpoints:	Lower set point: 21°C, Upper set point: 25°C (constant)	V: -ab 12 -ad $5{\cdot}10^4$ -lw $2{\cdot}10^{-6}$,
		Idealised: unlimited capacity and ideal response	D: -ab 2 -ad 10^3 -lw $5{\cdot}10^{-4}$ -c 3000
	System efficiencies (Beck et al. 2010)	η_e = 0.39 (electricity source to site eff. cooling), $\eta_{cool,deliv}$ = 0.7 (air system eff. cooling), COP_{cool} = 3, η_h = 0.95 (natural gas heating system eff.)	
		Anisotropic optical model for shade	s and D: MF3
		5 min. time step	hourly time step
Weather		IWEC, Amsterdam	

The magnitude of these errors can be decreased by increasing the number of window subdivisions. Within the daylight model, however, the number of subdivisions is proportional to the required computational effort. In EnergyPlus, errors could be introduced by an inappropriate application of the underlying models. The shade model in EnergyPlus explicitly describes heat and mass exchange between the air cavity, the shade, the zone, and the window. The chosen application of this model is therefore likely to give errors in convective solar gains.

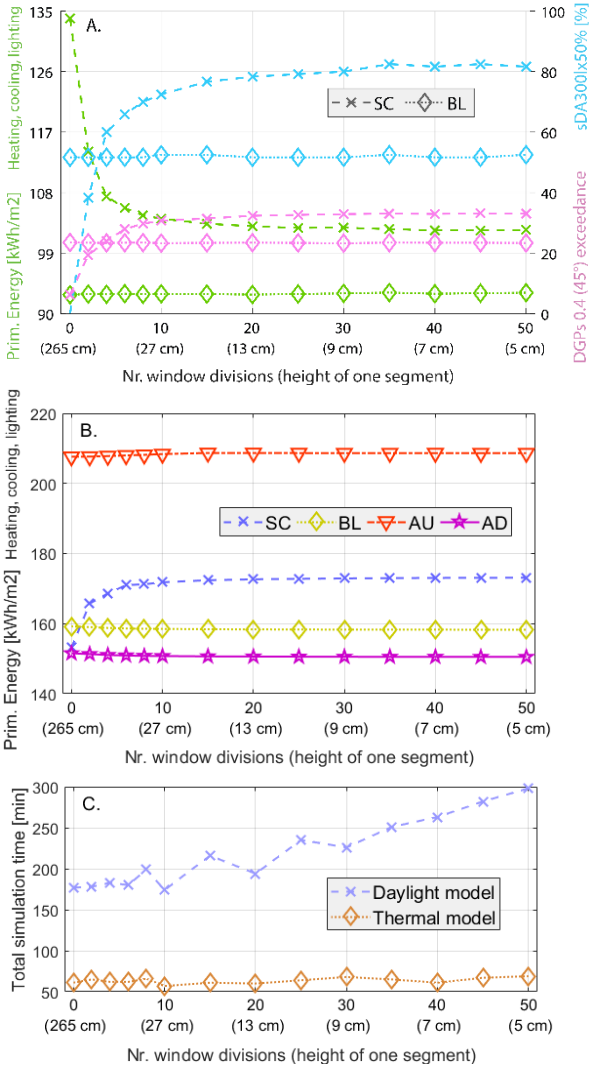

Figure 2 Sensitivity of results to window discretization. A. Daylight model, B. Thermal model, C. Sensitivity of simulation time for both models

Figure 2 presents a sensitivity analysis investigating an appropriate modelling resolution for the amount of window divisions. Figure 2 (A) shows the sensitivity of performance predictions by the daylighting model. Within Radiance, increasing window subdivisions will better approximate the amount of transmitted daylight, as is illustrated by the flattening of predicted performance for the SC case. Spatial daylight autonomy is the most sensitive indicator, flattening only at 35 divisions. Because simulation time increases strongly beyond this point (Figure 2 C) 35 divisions were chosen in this study. Figure 2 (B) shows the sensitivity of predicted primary energy consumption to the number of window divisions in EnergyPlus. In this analysis, daylight dimming of lighting was disabled. The AU and AD cases show that the errors introduced by the modelling approach have a small effect on performance predictions. The predicted performance of the SC strategy flattens out from 20 window divisions onward but for consistency 35 divisions was chosen in EnergyPlus.

Initial performance assessment of reference cases

Figure 3 compares the performance of the SC and BL strategies. In this graph, the performance indicators are reformulated so that the most desirable situation is found if all performance indicators are as low as possible. Primary energy consumption is expressed here as a percentage of the worst performing scenario (AD: 124 kWh/m^2). View and glare performance are shown as the share of occupied hours that their required criterion was not met. Daylighting performance is presented as the complementary percentage to sDA300/50: the floor area that does not receive at least 300 lux for 50% of occupied time. These results suggest that, although the SC strategy offers better daylighting performance, it does so at the expense of the other performance aspects. The reason for this is that the sun-tracking behaviour of the SC strategy causes the shade to be almost fully raised during mid-day in summer leading to unwanted solar heat gains as well a risk of glare from bright skies. These moments with bright sky conditions will be referred to as high-light conditions (Hi) from this point onward. A more beneficial trade-off between performance aspects might be found by lowering the shade further under these conditions.

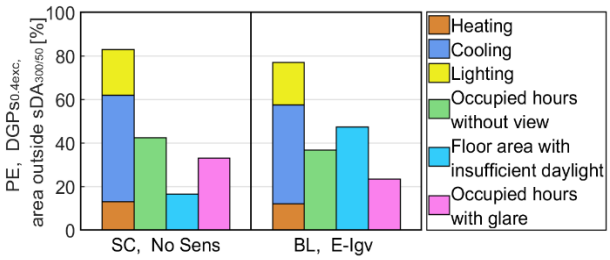

Figure 3 Summary of whole building performance for the SC and BL strategies

With the SC strategy, heating energy consumption is lower, but cooling and lighting are both higher than with the BL. Although lighting energy consumption is only 1% higher for the SC strategy than for the BL strategy this contrasts with the 26% increase in sDA300/50% that the SC strategy offers. The reason for this can be found in the spatial and temporal distribution of daylight, the illuminance cut-off criterion, and the chosen control approach for the artificial lighting system.

Regarding the temporal distribution of daylight; the contrast between lighting energy consumption and sDA300/50 suggests that the SC strategy offers less daylight at the moments which are most critical for lighting energy consumption. That is, moments with overcast sky conditions during the winter period. At such moments, referred to as moments with low-light conditions (Lo) from here onward, the low altitude of the sun causes the shade to be positioned rather low, leading

to an unnecessary decline in daylighting performance. At these instances, the risk of glare or undesirable solar gains are low. Fully raising the shade at these moments is thus a promising way to improve the SC strategy.

Development of sensor strategies through BPS

This section will explore how various sensor alternatives can be used to detect low-light and high-light conditions and presents a method for comparing the effectivity of the different sensors in doing so. The goal of the analyses presented here is to find a control threshold which corresponds sufficiently well with instances related to undesirable glare and daylighting performance without leading to many false control decisions. Figure 4 illustrates how the approach works for using the indoor illuminance sensor as an example. The graph explores how the sensor could be used to detect low-light conditions where the shade could be safely raised without causing disturbing glare. The graph is based on results from the AU case and it shows DGPs for the two viewing directions plotted as a function of what the indoor vertical illuminance sensor would measure. For each viewing direction, the plotted DGPs value is the maximum of both seating positions. Using this graph, the effectivity of a potential sensor threshold can be assessed. The goal is to detect the conditions with a risk of disturbing glare (points below the horizontal 0.4 DGPs line) using a sensor threshold which can be expressed as a vertical line. In this graph, the detection of glare risk is called a 'positive'. True positives (TP) are moments where the chosen threshold rightly detects such conditions, in this example the control would remain in sun-tracking mode. True negative (TN) refers to moments where the chosen threshold would rightly conclude that there is no risk of glare and the roller blind would be fully raised. False negatives (FN) and false positives (FP) refer to situations where the threshold would lead to wrong control decisions causing glare or unnecessary loss of daylight respectively. The effectivity of different control thresholds and sensors can therefore be expressed by the share of occupied hours that are contained in each region, where a higher share of moments in the 'true' regions indicate better performance trade-offs between daylighting performance and visual comfort.

In the example shown in Figure 4; the threshold is chosen such that false negatives, where raising the shade would cause glare, never occur. Here, the 45-degree viewing angle is used. This approach leads to a substantial number of false positives (11% of occupied hours). The linear relationship between glare and sensed illuminance, within the plotted range, suggests that a more desirable trade-off can be reached by shifting the threshold closer to point where the linear regression line intersects the disturbing glare line. This approach is illustrated by the second cross in Figure 4, where the threshold was determined by allowing DGPs 0.4 to be exceeded 2% of the time.

Using these two approaches, control thresholds detecting low light conditions were determined for each type of sensor. In Table 2 these thresholds are summarised along with the corresponding effectivity of each sensor strategy, expressed as the share of occupied hours spent within each 'true' or 'false' detection region. From this table, it can be concluded that the external horizontal irradiance sensor is less effective at detecting low light conditions than the other sensors. Additionally, these results show that the approach where 2% glare probability occurrence from 'false negatives' is accepted, offers much fewer 'false positives'. This suggests that this option offers a more desirable trade-off between daylight utilisation and glare probability.

A similar approach is used in choosing a threshold for the detection of high light conditions. Here a control action is meant to prevent glare in a situation where the control strategy would otherwise be tracking the sun. Therefore, simulation results from the SC strategy are used. Figure 5 (A) shows DGPs as a function of measured indoor illuminance. The cross marks the effects of using a control threshold which would detect a risk of glare at all times for a view facing the wall. The relationship between glare probability and measured illuminance is less linear than in the last example. The performance trade-off between glare and daylight utilisation is therefore also less beneficial, as can be seen by the high occurrence of false positives (35%). The lack of a linear relationship can be explained by the occurrence of glare associated with a large fraction of the window being exposed, exposing the occupant to a large view of a high luminance sky.

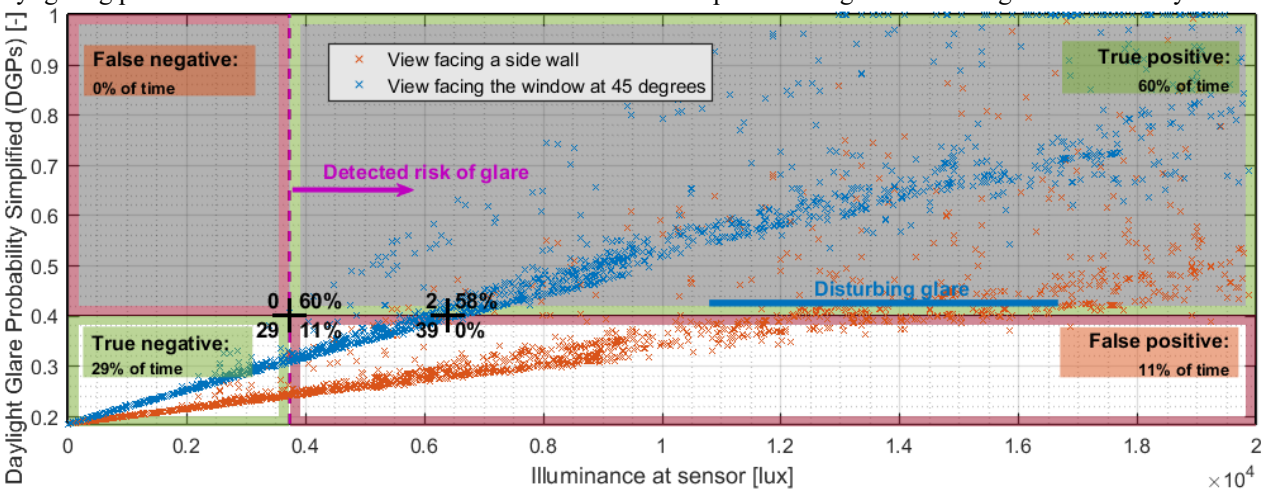

Figure 4 DGPs in relation to readings from the indoor vertical illuminance sensor. Simulated results for the AU case.

Table 2 Summary of sensor thresholds for detecting low light conditions using different sensors. F: false, T: true.

	Exterior horizontal irradiance sensor		**Exterior vertical irradiance sensor**		**Interior vertical illuminance sensor**	
	Negative	Positive	Negative	Positive	Negative	Positive
Threshold based on: $DGPs_{45\ deg} >= 0.4$	30 W/m²		50 W/m²		4000 lux	
	FN: 0%	TP: 60%	FN: 0%	TP: 60%	FN: 0%	TP: 60%
	TN: 17%	FP: 22%	TN: 31%	FP: 9%	TN: 29%	FP: 11%
Threshold based on: $DGPs_{45deg[2\%]} >= 0.4$	80 W/m²		80 W/m²		6400 lux	
	FN: 2%	TP: 58%	FN: 2%	TP: 58%	FN: 2%	TP: 58%
	TN: 29%	FP: 11%	TN: 39%	FP: 1%	TN: 39%	FP: 0%

A sensor strategy based on a luminance distribution at the position of the occupant would be the most ideal in this case. As such a strategy is faced with many practical obstacles, a promising direction might be to try to approximate similar behaviour using the more acceptable window sensor position. Figure 5 (B) gives an example of such an approach. Here the illuminance measured by the sensor is multiplied by the unshaded height of the window. The relationship between DGPs and this non-physical quantity is much more linear than in the case with measured illuminance. Consequently, the performance trade-off is more beneficial as can be seen by the lower occurrence of false positives (18%).

Table 3 give a summary of the developed thresholds, in relation to an assessment of their effectivity, for each of the sensor types. It can be seen that the approach where sensor measurements are multiplied by the unshaded height of the window, is generally more effective. The results suggest that the global horizontal irradiance sensor offers the worst performance if direct measurements are used. Surprisingly, however, this sensor appears to be the most favourable when the measurements are multiplied by the unshaded height of the window. This appears counterintuitive as the placement and measurement spectrum of the sensor has the least in common with the sensor that is used to assess glare. The explanation for these results is that, when the sun is not in view, the remaining occurrence of glare discomfort is strongly connected to the overall brightness of the sky. The two vertical sensors are less effective in measuring such an overall sky brightness as their measurements are more strongly influenced by the direct solar component.

Evaluation of the developed sensor strategies

To assess the effectivity of the different sensor types, only the most promising threshold approaches will be used.

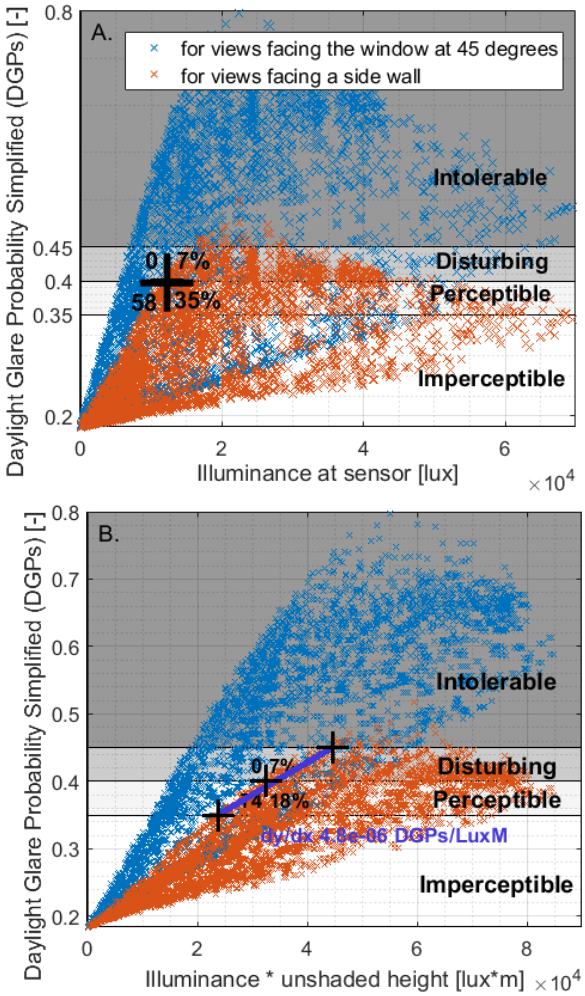

Figure 5 Simulated results from the SC case. DGPs in relation to: A. indoor vertical illuminance B. indoor vertical illuminance multiplied by the unshaded window height.

Table 3 Summary of sensor thresholds for detecting high light conditions using different sensors. F: false, T: true.

	Exterior horizontal irradiance sensor		**Exterior vertical irradiance sensor**		**Interior vertical illuminance sensor**	
	Negative	Positive	Negative	Positive	Negative	Positive
Threshold based on: $DGPs_{0\ deg} >= 0.40$	300 W/m²		150 W/m²		12300 lux	
	FN: 0%	TP: 7%	FN: 0%	TP: 7%	FN: 0%	TP: 7%
	TN: 69%	FP: 23%	TN: 57%	FP: 36%	TN: 58%	FP: 35%
Threshold based on: $DGPs_{0\ deg} >= 0.40$ and sensor value * unshaded height	760 (W/m²)·m		380 (W/m²)·m		32500 lux·m	
	FN: 0%	TP: 7%	FN: 0%	TP: 7%	FN: 0%	TP: 7%
	TN: 82%	FP: 11%	TN: 71%	FP: 21%	TN: 74%	FP: 18%

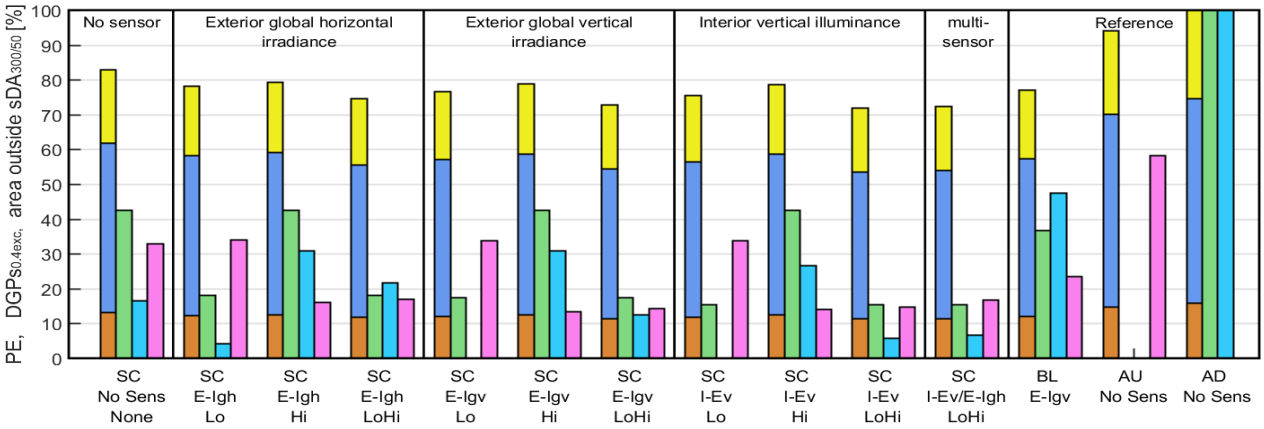

Figure 6 Summary of whole building performance for the improved SC strategy using different sensors. Lo: responds to low light condition, Hi: responds to low light condition, Performance indices defined as in Figure 3

Low light conditions will be detected using the thresholds where some occurrence of glare probability is accepted. High light conditions will be detected using the thresholds using the multiplication of measurements with the unshaded height of the window. In response to a low light condition being detected, the shade will be fully raised. In response to the detection of a high light condition, the control strategy will use the level of a seated occupant (1.2 meters) as a maximum height for the shade's position. To this end, the control strategy will use the minimum of the position following sun-tracking and 1.2 meters.

Figure 6 presents a summary of whole building performance for the developed control strategies and sensor alternatives. The performance indicators are defined as in Figure 3. For each sensor alternative, the effectivity in detecting low, and high light conditions is assessed by also evaluating scenarios where only one of the two proposed control extensions is implemented. For all sensor types we see a similar pattern in performance improvements. Compared to the initial SC strategy, fully raising the shade with low light conditions (Lo) improves daylighting and energy performance as well as the time with a view to the outdoors without causing a significant change in visual discomfort. The improvements in energy performance can be attributed to reductions in heating, lighting and even cooling energy consumption due to reduced lighting gains.

The control response to high light conditions improves overall energy performance and reduces the time that the visual discomfort criterion is met by 17-19%. These improvements do have a negative effect on daylighting performance (10-14% reduction in sDA). The implementation of both control modes has a beneficial effect on all performance aspects. Only in the case of the exterior outdoor horizontal irradiance sensor does this lead to a slight decline in daylighting performance in relation to the initial strategy. For all sensor types, the improved strategy shows superior performance over the conventional BL strategy in all performance indicators. Depending on which sensor is used, the improved strategy offers 1-4% reduction in primary energy consumption, 26-42% more floor area with sufficient daylight, 19-21% more occupied hours with a view and 6-9% less time with a probability of disturbing glare. Substantial differences can be observed between the three sensors, where the indoor illuminance sensor stands out as the best performing alternative for all performance indicators. The least performing sensor is the global horizontal irradiance sensor which scores worst for all indicators.

Conclusion

This simulation study showed that, using the proposed method, a sensor strategy for automated shading systems can be developed, resulting in significant improvements in terms of whole building performance over conventional shading control systems. The screening method identifies sensor thresholds associated to desirable building performance using only a very limited number of simulations. This offers opportunities for utilising this method within a framework meant for answering a broader range of questions. These could be focussed on the robustness of conclusions to occupant related uncertainties, as well as the sensitivity of the results to assumptions regarding the case study building.

Although this case study focussed on using discrete thresholds and actuations, more beneficial performance trade-offs might be found using proportional control responses, and the presented method can be applied in their development. For instance, rather than using a fixed maximum shade height under high light conditions, this maximum can be determined using the slope in Figure 5.

Within the case study, the indoor illuminance sensor was identified as the most desirable alternative in terms of building performance. This study also concludes that the performance prediction of a variable height shading strategy is particularly sensitive to the modelled number of fenestration divisions used to describe the variation in shade positions within EnergyPlus and the Radiance three-phase method.

The performance indicator that was used for glare calls for some caution in its interpretation. Although DGPs has been shown to be a reliable metric in cases where the sun is not in an occupant's field of view, this condition is not always met in all the cases presented in this study. Wienold (2009) and Konstantzos et al. (2016) have shown

that the perception of glare can occur due to direct sunlight being visible through a fabric roller shade. Additionally, direct sunlight is visible in the BL and AU reference scenarios. Although the DGPs can give different results than the more reliable image based DGP metric, Santos and Caldas (2018) have shown that these metrics are consistent in predicting the occurrence of instances which exceed the disturbing glare criterion (DGP/DGPs >0.4) used in this study. The choice for a glare metric should also be considered in relation to the uncertainty in the inputs required by the associated simulation methods. The increased reliability of the DGP metric, for instance, has to be weighed with the uncertainty associated to luminance-based glare assessments from simulations with a low-resolution BSDF and the required assumptions regarding façade design and interior layout. It can be concluded that fit-for-purpose glare performance prediction for the development of solar shading controls requires further research. The method presented in this paper, however, does not depend on the applied metric.

The use of hourly weather data in this study is reason for some reservations regarding its conclusions. In reality, sub-hourly outdoor daylight conditions show much more variability than what is represented by such data. Walkenhorst et al. (2002) have shown that the temporal interval of irradiance data can significantly influence simulated performance predictions of spaces equipped with daylight dimming systems and its influence is expected to be even stronger for automated shading systems. Although methods for the generation of synthetic sub-hourly weather data are available, the application of these methods to the Dutch climate and automated solar shading control has not been tested. This topic is considered a large uncertainty in the use of BPS for the development of dynamic shading solution and it is recommended for further research.

References

Atzeri, A., A. Gasparella, et al. (2018). Comfort and energy performance analysis of different glazing systems coupled with three shading control strategies. *Science and Technology for the Built Environment 24(5)*: 545-558.

Beck, W. (edited by), D. Dolmans, et al. (2010). *Solar Shading. REHVA Guidebook 12*, REHVA. Forssa.

Bueno, B., J. Wienold, et al. (2015). Fener: A Radiance-based modelling approach to assess the thermal and daylighting performance of complex fenestration systems in office spaces. *Energy and Buildings 94*: 10-20.

D'Antoni, M., P. Bonato, et al. (2019). IEA SHC Task 56 - System Simulation Models, part C Office Buildings. Paris, France, International Energy Agency.

Jeong, K., A. Choi, et al. (2016). A mock-up study for validation of an improved control algorithm for automated roller shade. *Indoor and Built Environment 25(1)*: 17-28.

Konstantzos, I., A. Tzempelikos, et al. (2016). Daylight Glare Evaluation When the Sun is Within the Field of View Through Window Shades.

Koo, S., M. Yeo, et al. (2010). Automated blind control to maximize the benefits of daylight in buildings. *Building and Environment 45(6)*: 1508-1520.

Loonen, R. (2018). Approaches for computational performance optimization of innovative adaptive façade concepts. *Doctoral thesis*, Eindhoven University of Technology.

Loonen, R., F. Favoino, et al. (2017). Review of current status, requirements and opportunities for building performance simulation of adaptive facades. *Journal of Building Performance Simulation 10(2)*: 205-223.

McNeil, A. and E.S. Lee (2013). A validation of the Radiance three-phase simulation method for modelling annual daylight performance of optically complex fenestration systems. *Journal of Building Performance Simulation 6(1)*: 24-37.

Santos, L. and L. Caldas (2018). Assessing the Glare Potential of Complex Fenestration Systems: a Heuristic Approach Based on Spatial and Time Sampling. *Passive and Low Energy Architecture 2018*. Hong Kong, China.

Seong, Y.B., M.S. Yeo, et al. (2014). Optimized control algorithm for automated venetian blind system considering solar profile variation in buildings. *Indoor and Built Environment 23(6)*: 890-914.

Shen, E., J. Hu, et al. (2014). Energy and visual comfort analysis of lighting and daylight control strategies. *Building and Environment 78*: 155-170.

Shen, H. and A. Tzempelikos (2012). Daylighting and energy analysis of private offices with automated interior roller shades. *Solar energy 86(2)*: 681-704.

Subramaniam, S. (2017). Daylighting Simulations with Radiance using Matrix-based Methods.

Tzempelikos, A. and H. Shen (2013). Comparative control strategies for roller shades with respect to daylighting and energy performance. *Building and Environment 67*: 179-192.

Walkenhorst, O., C. Reinhart, et al. (2002). Dynamic annual daylight simulations based on one-hour and one-minute means of irradiance data. *Solar Energy 72(5)*: 385-395.

Werner, M., D. Geisler-Moroder, et al. (2017). DALEC– a novel web tool for integrated day-and artificial light and energy calculation. *Journal of Building Performance Simulation 10(3)*: 344-363.

Wienold, J. (2007). Dynamic simulation of blind control strategies for visual comfort and energy balance analysis. *Building Simulation 2007*, Beijing, China

Wienold, J. (2009). Dynamic daylight glare evaluation. *Building Simulation 2009*, Glasgow, Scotland